

# Design and Optimization of an advanced time-of-flight neutron spectrometer for deuterium plasmas of the Large Helical Device <sup>a)</sup>

Yimo Zhang,<sup>1</sup> Lijian Ge,<sup>1</sup> Zhimeng Hu,<sup>1,3</sup> Jiaqi Sun,<sup>1</sup> Xiangqing Li,<sup>1</sup> Kunihiro Ogawa,<sup>2</sup> Mitsutaka Isobe,<sup>2</sup> Siriyaoporn Sangaroon,<sup>2</sup> Longyong Liao,<sup>1</sup> Danke Yang,<sup>1</sup> Giuseppe Gorini,<sup>3,4</sup> Massimo Nocente,<sup>3,4</sup> Marco Tardocchi,<sup>4</sup> Tieshuan Fan<sup>1,b)</sup>

<sup>1</sup>State Key Laboratory of Nuclear Physics and Technology, Peking University, Beijing 100871, China

<sup>2</sup>National Institute for Fusion Science, 322-6 Oroshi-cho, Toki 509-5292, Japan

<sup>3</sup>Dipartimento di Fisica ‘G. Occhialini’, Università degli Studi di Milano-Bicocca, Milano 20126, Italy

<sup>4</sup>Institute for Plasma Science and Technology, National Research Council, Milan 20125, Italy

(Presented XXXXX; received XXXXX; accepted XXXXX; published online XXXXX)

(Dates appearing here are provided by the Editorial Office)

A time-of-flight neutron spectrometer based on the TOFED concept has been designed and is under development for the Large Helical Device (LHD). It will be the first advanced neutron spectrometer to measure the 2.5 MeV D-D neutrons (DDN) from helical/stellarator plasmas. The main mission of the new TOFED is to study the energetic ion behaviours in helical plasmas, which includes both deuterons from the auxiliary heating systems and tritons born from the d+d fusion reactions. The latter are measured by the triton burn-up neutrons (TBN) and the new spectrometer, unlike the original TOFED in the EAST tokamak, has been optimized for this scope. Based on Monte Carlo simulation by a GEANT4 model, the energy resolutions for DDN and TBN are 6.6% and 9.0%, respectively. The new TOFED is expected to be installed in the basement under the LHD hall, and shares the collimator with one channel of the neutron camera, which defines a vertical line-of-sight. The distance from the first scintillators of the new TOFED to the equatorial plane of LHD plasmas is about 15.5 meters. When projected to the neutron rates that are typically obtained in LHD deuterium plasmas, (order of  $10^{15}$  n/s with neutral beam injection) we expect to obtain the DDN and TBN counting rates of about 250 kHz and 250 Hz, respectively. This will make the simultaneous study of fast deuterons and fusion born tritons with neutron spectroscopy possible on time scales of few seconds, for the first time in helical/stellarator plasmas.

書式を変更: イタリア語 (イタリア)

## I. INTRODUCTION

Neutrons produced from D-D and D-T reactions carry the information about the kinematic state of fusion fuels in plasmas. Among magnetic confined fusion devices like tokamaks, the neutron diagnostics have been widely adopted<sup>1</sup>. Particularly in particular, the advanced Neutron Emission Spectroscopy (NES) diagnostics, such as the MPR<sup>2</sup> and the time-of-flight neutron spectrometer TOFOR<sup>3</sup> at the JET Joint European Torus, have been proved as proved to be powerful tools among instruments to understand the behavior of energetic particles<sup>4-8</sup> in fusion experiments, which is one of the most concerned issues in the ITER burning plasma physics of relevance for burning plasma devices, such as ITER<sup>9,10</sup>. With regard to the present stellarators and helical devices, the Large Helical Device (LHD) has firstly initiated started its first deuterium experimental campaigns from campaign in 2017, in order to explore the related fusion plasma physics and engineering

problems<sup>11</sup> challenges<sup>11</sup>. There are already rather comprehensive neutron diagnostics at the LHD, including neutron flux monitors, neutron activation systems, a vertical neutron camera, and scintillating-fiber detectors, which all operate with good performance during the recent experiments<sup>12</sup>. The recorded neutron emission rates at the LHD reach more than  $10^{15}$  n/s<sup>13</sup>, due to a large number of fast ions, mainly generated from the external power by the auxiliary heating system.

For studying the fast ion behaviours in order to advance our knowledge on the fast ion behaviour in the helical fusion plasmas, a new advanced time-of-flight neutron spectrometer based on the TOFED (Time-Of-Flight Enhanced Diagnostics) concept<sup>14</sup> is projected to will be developed at the LHD, which will and it will be the first advanced neutron spectrometer for the a helical/stellarator plasmas. The TOFED neutron spectrometer, which originates from the TOFOR concept but retains has an improved the optimized efficiency and energy resolution due to its double-ring secondary scintillator array, has been developed and put into successful operations at the EAST tokamak for diagnosing the studies of fast ions from the NBI (Neutral Beam Injection) and ICRF (Ion Cyclotron Resonance Frequency) heating plasmas<sup>15</sup> systems<sup>18</sup>. Moreover, time-resolved triton burn-up diagnosis have been

書式を変更: 上付き/下付き (なし)

<sup>a)</sup>Published as part of the Proceedings of the Virtual 23<sup>rd</sup> Topical Conference on High-Temperature Plasma Diagnostics (HTPD) hosted by Los Alamos National Laboratory.

<sup>b)</sup>Author to whom correspondence should be addressed: tsfan@pku.edu.cn

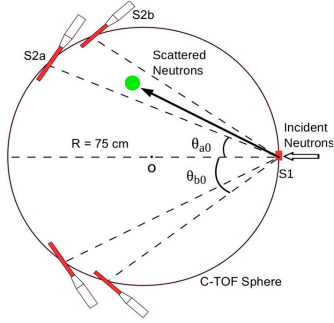


Fig. 1 The principle of the TOFED concept is exhibited shown. The primary scintillators S1 and the secondary scintillators S2 are arranged on the surface of the CTOF sphere. If When the collimated neutron flux perpendicularly hit the S1 scintillator, some neutrons will be deflected to the S2 detectors and their interaction recorded. Under these circumstances, the the protons inside the S1 and then scatter to the S2; the time-of-flight of scattering the scattered neutrons are is only determined by the incident neutrons energy, regardless of the different flight route path scattered neutrons may follow from S1 to S2.

conducted by the measurements of the 14 MeV D-T neutrons, such as using the scintillating-fiber detectors. According to the recent experimental results at LHD, the Triton Burnup Neutrons (TBN) yields exceed  $10^{12}$  n/s, up to 0.5% of the D-D neutrons (DDN)<sup>19</sup>. It will be an attractive application of the TOFED-type neutron spectrometer at the LHD if this new instrument can appropriately respond to both DDN and TBN from the helical fusion plasmas.

In this paper, the new TOFED neutron spectrometer at the LHD will be described. Section II briefly introduces the basic principle of the neutron time-of-flight measurement. In section III, the TOFED-type spectrometer concept at the LHD is discussed in detail. These results are summarized in the last section.

## II. TIME-OF-FLIGHT PRINCEPLEPRINCIPLE

The time-of-flight (TOF) neutron spectrometer consists of two sets of scintillators, see Figure 1. Assumed Assuming that all the scintillators are tangential to a sphere (with a radius  $R$ ) at their centers, the collimated neutrons hit the primary scintillators (S1) at the center along the diameter of the sphere. If one neutron with the energy  $E_n$  collides with one proton inside has a single scattering collision with a proton in S1, i.e., for just one time by an elastic scattering process  $n + p \rightarrow p_r + n'$ , in which the neutron scattering angle is  $\theta$ , the flight time  $t_{tof}$  for the scattering neutron to collide again inside the secondary scintillator (S2) can be derived from and then reaches the S2 scintillators, we have

$$t_{tof} = \frac{2R \cos \theta}{v_n'}, \quad (1)$$

$$E_n' = E_n \cos^2 \theta = \frac{m_n v_n'^2}{2}, \quad (2)$$

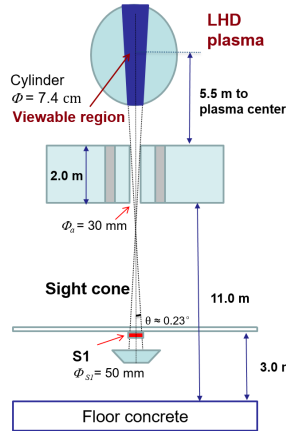


Fig. 2 The LHD-TOFED is expected to be installed under the LHD plasmas. A hole with a radius of 30 mm through the 2-meters-thick basement is used as the collimator and radiation shielding. The distance from the equatorial plane of LHD plasmas to the S1 scintillator of LHD-TOFED is at least 15.5 m. This collimator, which is originally used by the vertical neutron camera, defines a line-of-sight with a divergence of no more than 0.23°, and gives LHD-TOFED a viewable region which can be approximately regarded as a cylinder with a radius of about 7.4 cm.

Where  $\theta$  is the scattering angle,  $v_n'$  means is the velocity of the neutron after the first scattering, and  $m_n$  is the mass of the neutron and  $t_{of}$  denotes the time of flight. Therefore, energies of the incident neutron and the recoil proton inside the S2,  $E_n$  and  $E_p$ , can be denoted as are obtained as

$$E_n = \frac{2m_n R^2}{t_{tof}^2}, \quad (3)$$

$$E_p = E_n \sin^2 \theta = \frac{2m_n R^2}{t_{tof}^2} \sin^2 \theta, \quad (4)$$

which This implies that means that the scattering neutrons scattered neutrons born from incoming neutrons with the same energy  $E_n$  take the same time to will spend equal time to reach the identical spherical surface despite of S2 irrespective of their scattering angle  $\theta$  the different scattering angle. This is the so-called constant time-of-flight (CTOF) sphere principle. But the nNeutrons scattering multiple times inside the S1 would not obey will however break this principle the CTOF principle<sup>20</sup>. As shown in Fig. 1, the two rings of the TOFED's S2 scintillators cover a certain range of neutron scattering angles, thus determining the  $E_p$  collected by the S1 a range for the scattered proton energy  $E_p$  that can be released in S1, given  $E_n$ . The effective neutron events can thus be discriminated from the multiple events or carbon scattering events by the time-of-flight and recoiled proton energy, which constitutes the fundament principle of the double kinematic selection (DKS) method<sup>15,21</sup>. In the TOFED case, the radius of the CTOF is

書式を変更: フォント : Symbol

書式を変更: 下付き

書式を変更: 下付き

書式を変更: フォント : Symbol

1.5 m, and the range of the scattering angles is  $20^\circ < \theta < 31^\circ$  for S2a and  $31^\circ < \theta < 40^\circ$  for S2b, respectively.

### III. TOFED-TYPE SPECTROMETER AT THE LHD

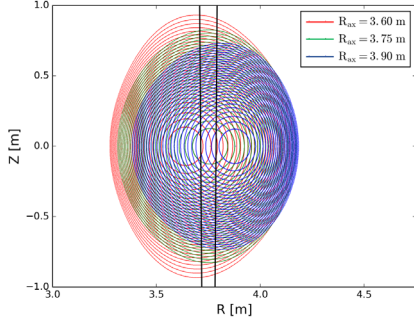


Fig. 3 The line-of-sight of the LHD-TOFED gives an approximately cylindrical ~~viewable-viewing~~ region (between the black lines). For the three typical magnetic configurations ( $R_{ax}=3.6$  m in red,  $R_{ax}=3.75$  m in green, and  $R_{ax}=3.9$  m in blue), the LHD-TOFED can always collect the fusion neutrons from the helical plasmas core.

The LHD is one of the largest superconducting helical device with a major radius/ minor radius of 3.9 m/ $\sim$ 0.6 m. Its NBI heating system consists of three tangentially-injected neutral beams with maximum beam energy of around 180 keV and 60 keV, respectively, and the total NBI power can be up to 30 MW. Besides, the ICRF system with total power of about 6 MW is also a main heating source at the LHD<sup>12</sup>. Analyzing the neutron spectra to obtain the kinematic states of the fuel ions, the TOFED-type neutron spectrometer (mentioned as LHD-TOFED in the later sections) is primarily aimed ~~at the research of the substantial~~ ~~at studying~~ fast ions ~~induced-produced~~ by these auxiliary heating in the LHD plasmas.

#### A. Line of sight

The ~~defined~~-LHD-TOFED is expected to be installed in the basement under the LHD hall, and shares one of the collimators ~~belonged-belonging~~ to the middle channel of the vertical neutron camera, ~~with a view line that passes going through the-a concrete shielding~~. The distance from the equational plane of LHD plasma to the S1 scintillator of LHD-TOFED is at least 15.5 m, as drawn in Fig. 2. This collimator with a radius of 30 mm defines a line-of-sight with a divergence of no more than  $0.23^\circ$ , and gives LHD-TOFED a ~~viewable-viewing~~ region which ~~can-beis~~ approximately ~~regarded-as~~ a cylinder with a radius of about 7.4 cm. ~~Despite that the rotational LHD plasma, the p~~The plasma profile observed by the LHD-TOFED ~~can-be treated-as-anis approximately an ellipse of-which-major-axis is-vertical-with a vertical major axis~~.

In LHD, ~~the~~ the magnetic configuration can be shifted ~~outwardly or inwardly~~ ~~outward or inward~~ as illustrated in Fig. 3. During the typical operation regime at the LHD, the radii of the magnetic axis usually range from 3.6 m to 3.9 m. ~~On this condition~~ ~~In these conditions~~, the line-of-sight of the new instrument (black line) can always ensure the observation of a collimated line-integrated neutron flux from ~~the helical plasma-core~~ ~~plasma core of the helical plasma~~.

TABLE I. The main technical parameters of the APV8104-14 digitizer.

Sampling rate	Number of channels	Bit number	$V_{pp}$	bandwidth	RAM
1 Gs/s	4	14	$\pm 3$ V	500 MHz	2 GB

#### B. Data Acquisition

The ~~D~~igital DAQ (data acquisition) system ~~envisaged for the LHD-TOFED is based on the-compat digitizers is compact-and-able-to~~ ~~that can acquire various information about the nuclear events at the same time, such as the triggering time and pulse height of the neutron pulses~~ ~~measure the pulse height and time information of neutron scattering events in S1 and S2~~. In recent experiments, ~~various-several~~ NES diagnostics ~~at the tokamaks in tokamaks~~ around the world have upgraded the electronics through the employment of digitizers<sup>22-24</sup>. ~~We have chosen a candidate digitizer (The APV8104-14 from Techno AP) as been chosen as the reference for the LHD-TOFED~~. Its main features and parameters are listed in TABLE I. The communication between this type of digitizer and the computer is established by the TCP/IP protocol. The digital DAQ system can ~~be fairly tolerable of counting rates in orders~~ ~~work at counting rates up to-of~~ 1 MHz at the LHD due to the 2 GB RAM and the data transmission by optical fibers. ~~It is validated that the-A~~ sampling rate of 1 G samples/s satisfies the requirements of sub-nanosecond level precision for neutron time-of-flight measurements, combined with the CFD (Constant Fraction Discrimination) method in the off-line data processing<sup>18,22</sup>. The mix mode for data acquisition can collect both the pulse shape and triggering time, making it possible to apply the DKS method to ~~improving-improve~~ the signal-to-noise of the neutron time-of-flight spectra. ~~More d~~Detailed ~~work-tests on-of~~ the digital DAQ system will be conducted in the future.

#### C. Response to DDN and TBN

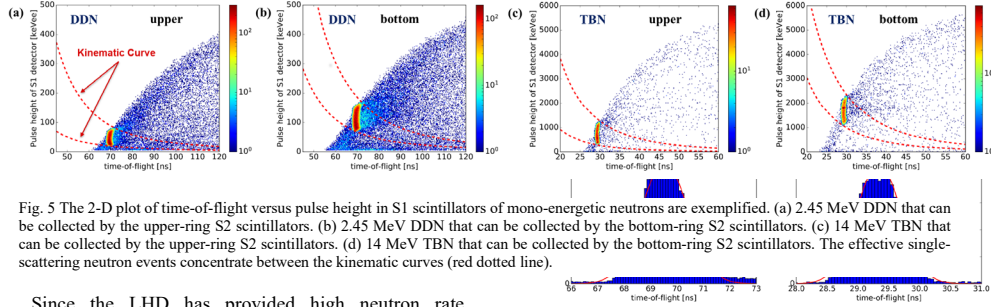


Fig. 5 The 2-D plot of time-of-flight versus pulse height in S1 scintillators of mono-energetic neutrons are exemplified. (a) 2.45 MeV DDN that can be collected by the upper-ring S2 scintillators. (b) 2.45 MeV DDN that can be collected by the bottom-ring S2 scintillators. (c) 14 MeV TBN that can be collected by the upper-ring S2 scintillators. (d) 14 MeV TBN that can be collected by the bottom-ring S2 scintillators. The effective single-scattering neutron events concentrate between the kinematic curves (red dotted line).

Since the LHD has provided high neutron rate comparable to that at large tokamaks like JET, considerable triton burnup neutrons would be emitted from its helical plasmas. A Monte Carlo model is developed by means of the neutron transport simulation from the plasma to the LHD-TOFED has been developed using the GEANT code<sup>25</sup> for the LHD-TOFED. In the simulation, the scintillators of both S1 (EJ228) and S2 (EJ200) keep unchanged from the original are the same as those of the original TOFED. The performances of two kinds-type of scintillators are have been previously investigated and their light output function is calibrated by known from calibration experiments at the accelerator neutron accelerators<sup>15,16</sup>. Its responses to both

single-time-scattered on neutron inside the S1 obey the

Fig. 4 The simulated time-of-flight spectra for mono-energetic (a) 2.45 MeV and (b) 14 MeV neutrons are shown. The Gaussian fitting curves are plotted in red.

equation (4) and depends on the range of the neutron scattering angle, and thus the scintillation light output induced by these protons are restricted by the scattering angles of neutrons. In the 2D figure of time-of-flight versus pulse height of the protons in the S1, pictured shown in Fig. 5, we find that the effective single scattering neutron events concentrate between the two kinematic curves. These, which depend only on the finite scattering angle range

TABLE II. The energy resolutions of LHD-TOFED for DDN and TBN.

$E_n$ [MeV]	$t_{tof}$ [ns]	FWHM from geometry[ns]	FWHM from light propagation [ns]	FWHM from DAQ [ns]	Energy resolution [%]
2.45	69.5	2.09	0.6	0.5	6.6
14.0	29.3	1.88	0.6	0.5	9.0

the 2.5 MeV DDN and the 14 MeV TBN emission are has been also evaluated.

The overall geometry of the scintillator array of LHD-TOFED is responsible for a Gaussian shape broadening of the time of flight spectrum resulting from a collimated beam of 2.5 MeV monoenergetic neutrons as input. Collimated mono-energetic neutrons bring a Gaussian-shaped time-of-flight spectrum in the simulation due to the geometry of the scintillator array in the LHD-TOFED. The fitting results by fitting the simulations results, we obtain show that the DDN peak on  $t_{tof}$ -axis is located at around 69.5 ns, while the TBN peak at 29.3 ns, as shown in Fig. 4. The FWHMs for DDN and TBN spectra are 2.09 ns and 1.88 ns, respectively. Accounting the contributions by also taking into account the contribution from by the digital DAQ system and light transmission from the scintillators to the photo multiplier tube, the total energy resolutions are determined to be of the integrated neutron spectrometer would be about 6.6% for DDN and 9.0% for TBN, respectively. The More details on the contribution of each term to the overall of energy resolutions of the instrument are given in TABLE II.

As far as the energy released by single scattered protons in S1 is concerned, this is determined by Energy of protons

determined by the solid angle covered by S2, only rely on the fixed range of the scattering angles due to the finite solid angle covered by the S2. Therefore, a lot of multiple most of the multiple scattering events, or those due single scattering on carbon-scattering events can be filtered by the DKS method. We note that the discrimination capability based on the DKS method is higher for 14 MeV TBN than 2.45 MeV DDN events, which implies an even better single-to-noise ratio of TBN measurements. The proportion of the false 2.45-MeV DDN events are significantly higher than that of 14-MeV TBN, so the DKS method can give even better signal-to-noise ratio to measure the TBN for the helical plasmas. For the separate ring of the S2 scintillators, the range of proton energy deposited in S1 scintillators from the protons are different due to the different coverages of neutron scattering angles. The larger pulse height for the bottom ring is owing to the larger neutron scattering angles. By considering the finite geometry of S2, we expect that energies in the range. Meanwhile, it can be learned that pulse heights of the effective events range from about 20 keVee to 180 keVee for the DDN, and from about 300 keVee to 2300 keVee for the TBN may be deposited in the S2 scintillators. It demands that the digitizers. Hence, there is need for in the DAQ system with a have dynamic range of

TABLE III. The estimated neutron counting rates for DDN and TBN at the primary scintillators of the LHD-TOFED.

Neutron type	Neutron Flux [n/s·cm <sup>2</sup> ]	Area efficiency [cm <sup>2</sup> ]	Counting Rate [kHz]
DDN	10 <sup>6</sup>	0.25	250
TBN	5·10 <sup>3</sup>	0.05	0.25

3 orders of magnitude and with high signal-to-noise ratio, which is necessary for the LHD-TOFED to measure to measured simultaneously the DDN and TBN emission simultaneously with the LHD-TOFED.

During the recent experimental campaigns at LHD, it was confirmed that the neutron yield can reach more than  $1 \times 10^{15}$  n/s and the TBN ratio can be up to 0.5%. With the expected vertical-line-of sight, the neutron fluxes on S1 scintillators of the LHD-TOFED are estimated to be  $10^6$  n/s·cm<sup>2</sup> for DDN and  $5 \cdot 10^3$  n/s·cm<sup>2</sup> for TBN. Considering the detection efficiency presented in TABLE III, the recorded counting rates of registered DDN and TBN could be 250 kHz and 250 Hz, respectively, in which the count rates is possibly sufficient for the diagnosis of the This will allow studies of the DDN and TBN emission on time scales of 1/10 and some seconds for the two components, respectively. It demonstrates the feasibility of NES diagnosis by the LHD-TOFED, and additionally, the neutron spectrometer might have the potentially application as the auxiliary diagnostic of TBN ratio on time scales of few seconds in the helical fusion plasmas at the LHD.

#### IV. CONCLUSION

A TOFED-type neutron spectrometer (LHD-TOFED) is introduced and is under development at for the LHD and will, and it will be the first NES diagnostic in a helical/stellarator device. The main mission of the LHD-TOFED is to measure the 2.5 MeV D-D neutrons for diagnosing energetic ion behaviors in the helical/stellarator plasmas, with the additional capability to measure 14 MeV neutrons born in triton burn up reactions. Its capability of measuring the TBN is also evaluated. By using a Based on the digital data acquisition system and a double kinematic selection method, application of DKS method can well optimize the a sufficient signal-to-noise ratio for measuring both simultaneously the DDN and TBN components can be obtained. It also demonstrates that the LHD-TOFED not only can be used for the diagnosis of fast deuterons, but also indicates the potential as an auxiliary diagnostic for the 14 MeV TBN ratio on time scales of few seconds in the helical plasmas at the LHD during the typical experiment regime with high NBI power delivered. The LHD-TOFED will be one of the main diagnostics for studies of fast ions in deuterium helical plasmas at LHD and will also serve as a complementary diagnostics for investigations on the confinement of MeV range tritons born in DD fusion reactions.

#### ACKNOWLEDGMENTS

This work was supported by the National MCF Energy R&D Program (Nos. 2019YFE03040000, 2013GB106004 and 2012GB101003), the National Key Research and Development Program of China (Nos. 2016YY0200805 and 2017YFF0206205), the State Key Program of National Natural Science of China (No. 11790324), and the User with Excellence Program of Hefei Science Center CAS (No. 2020HSC-UE012). The authors are very grateful to the EAST operation team for their help during the experimental campaigns.

<sup>1</sup>B. Wolle, Phys. Rep. **312**, 1 (1999).

<sup>2</sup>G. Ericsson, L. Ballabio, S. Conroy, J. Frenje, H. Henriksson, A. Hjalmarsson, J. Källne, and M. Tardocchi, Rev. Sci. Instrum. **72**, 759 (2001).

<sup>3</sup>M. Gatu Johnson, L. Giacomelli, A. Hjalmarsson, J. Källne, M. Weiszflog, E. Andersson Sundén, S. Conroy, G. Ericsson, C. Hellesen, E. Ronchi, H. Sjöstrand, G. Gorini, M. Tardocchi, A. Combo, N. Cruz, J. Sousa, and S. Popovichev, Nucl. Instruments Methods Phys. Res. Sect. A Accel. Spectrometers, Detect. Assoc. Equip. **591**, 417 (2008).

<sup>4</sup>J. Källne, L. Ballabio, J. Frenje, S. Conroy, G. Ericsson, M. Tardocchi, E. Traneus, and G. Gorini, Phys. Rev. Lett. **85**, 1246 (2000).

<sup>5</sup>C. Hellesen, M. Albergante, E.A. Sundén, L. Ballabio, S. Conroy, G. Ericsson, M.G. Johnsson, L. Giacomelli, G. Gorini, A. Hjalmarsson, I. Jenkins, J. Källne, E. Ronchi, H. Sjöstrand, M. Tardocchi, I. Voitsekhovitch, M. Weiszflog, and J.-E. contributors, Plasma Phys. Control. Fusion **52**, 085013 (2010).

<sup>6</sup>C. Hellesen, M. Gatu Johnson, E. Andersson Sundén, S. Conroy, G. Ericsson, J. Eriksson, H. Sjöstrand, M. Weiszflog, T. Johnson, G. Gorini, M. Nocente, M. Tardocchi, V.G. Kiptily, S.D. Pinches, and S.E. Sharapov, Nucl. Fusion **53**, 113009 (2013).

<sup>7</sup>J. Eriksson, M. Nocente, F. Binda, C. Cazzaniga, S. Conroy, G. Ericsson, L. Giacomelli, G. Gorini, C. Hellesen, T. Hellsten, A. Hjalmarsson, A.S. Jacobsen, T. Johnson, V. Kiptily, T. Koskela, M. Mantsinen, M. Salewski, M. Schneider, S. Sharapov, M. Skiba, M. Tardocchi, and M. Weiszflog, Nucl. Fusion **55**, (2015).

<sup>8</sup>C. Hellesen, M. Mantsinen, S. Conroy, G. Ericsson, J. Eriksson, V.G. Kiptily, and F. Nabais, Nucl. Fusion **58**, 123026 (2018).

<sup>9</sup>N.N. Gorelenkov, S.D. Pinches, and K. Toi, Nucl. Fusion **54**, 125001 (2014).

<sup>10</sup>M. Nocente, J. Fusion Energy **38**, 291 (2019).

<sup>11</sup>M. Osakabe, Y. Takeiri, T. Morisaki, G. Motojima, K. Ogawa, M. Isobe, M. Tanaka, S. Murakami, A. Shimizu, K. Nagaoka, H. Takahashi, K. Nagasaki, H. Takahashi, T. Fujita, Y. Oya, M. Sakamoto, Y. Ueda, T. Akiyama, H. Kasahara, S. Sakakibara, R. Sakamoto, M. Tokitani, H. Yamada, M. Yokoyama, and Y. Yoshimura, Fusion Sci. Technol. **72**, 199 (2017).

<sup>12</sup>M. Isobe, K. Ogawa, T. Nishitani, H. Miyake, T. Kobuchi, N. Pu, H. Kawase, E. Takada, T. Tanaka, S. Li, S. Yoshihashi, A. Uritani, J. Jo, S. Murakami, and M. Osakabe, IEEE Trans. Plasma Sci. **46**, 2050 (2018).

<sup>13</sup>K. Ogawa, M. Isobe, T. Nishitani, R. Seki, H. Nuga, S. Murakami, M. Nakata, N. Pu, M. Osakabe, J. Jo, M. Cheon, J. Kim, G. Zhong, M. Xiao, and L. Hu, Plasma Phys. Control. Fusion **60**, 095010 (2018).

<sup>14</sup>X. Zhang, Z. Chen, X. Peng, Z. Hu, T. Du, Z. Cui, X. Xie, X. Yuan, T. Fan, J. Källne, G. Gorini, M. Nocente, M. Tardocchi, L. Hu, G. Zhong, S. Lin, B. Wan, X. Li, G. Zhang, and J. Chen, Nucl. Fusion **54**, 104008 (2014).

<sup>15</sup>X.Y. Peng, Z.J. Chen, X. Zhang, Z.M. Hu, T.F. Du, Z.Q. Cui, X.F. Xie, L.J. Ge, X. Yuan, G. Gorini, M. Nocente, M. Tardocchi, L.Q. Hu, G.Q. Zhong, S.Y. Lin, B.N. Wan, X.Q. Li, G.H. Zhang, J.X. Chen, and T.S. Fan, Rev. Sci. Instrum. **85**, 11E112 (2014).

<sup>16</sup>X.Y. Peng, Z.J. Chen, X. Zhang, T.F. Du, Z.M. Hu, L.J. Ge, Y.M. Zhang, J.Q. Sun, G. Gorini, M. Nocente, M. Tardocchi, L.Q. Hu, G.Q. Zhong, N. Pu, S.Y. Lin, B.N. Wan, X.Q. Li, G.H. Zhang, J.X. Chen, and T.S. Fan, Rev. Sci. Instrum. **87**, 11D836 (2016).

<sup>17</sup>L.J. Ge, Z.M. Hu, Y.M. Zhang, J.Q. Sun, X. Yuan, X.Y. Peng, Z.J. Chen, T.F. Du, M. Nocente, G. Gorini, M. Tardocchi, L.Q. Hu, G.Q. Zhong, B.N. Wan, X.Q. Li, and T.S. Fan, Rev. Sci. Instrum. **89**, 101143 (2018).

<sup>18</sup>Y. Zhang, Ph.D. thesis, Peking University, in Chinese (2020).

<sup>19</sup>K. Ogawa, M. Isobe, T. Nishitani, S. Murakami, R. Seki, M. Nakata, E. Takada, H. Kawase, and N. Pu, Nucl. Fusion **58**, 034002 (2018).

<sup>20</sup>G. Gorini and J. Källne, Rev. Sci. Instrum. **63**, 4548 (1992).

<sup>21</sup>X. Zhang, J. Källne, G. Gorini, M. Nocente, T. Fan, X. Yuan, X. Xie, and Z. Chen, Rev. Sci. Instrum. **85**, 043503 (2014).

<sup>22</sup>Z.J. Chen, X.Y. Peng, X. Zhang, T.F. Du, Z.M. Hu, Z.Q. Cui, L.J. Ge, X.F. Xie, X. Yuan, G. Gorini, M. Nocente, M. Tardocchi, L.Q. Hu, G.Q. Zhong, S.Y. Lin, B.N. Wan, X.Q. Li, G.H. Zhang, J.X. Chen, and T.S. Fan, Rev. Sci. Instrum. **85**, 11D830 (2014).

<sup>23</sup>M. Skiba, G. Ericsson, A. Hjalmarsson, C. Hellesen, S. Conroy, E. Andersson-Sundén, J. Eriksson, and JET Contributors, Nucl. Instruments Methods Phys. Res. Sect. A Accel. Spectrometers, Detect. Assoc. Equip. **833**, 94 (2016).

<sup>24</sup>L.J. Ge, Z.M. Hu, Y.M. Zhang, J.Q. Sun, X. Yuan, X.Y. Peng, Z.J. Chen, T.F. Du, G. Gorini, M. Nocente, M. Tardocchi, L.Q. Hu, G.Q. Zhong, S.Y. Lin, B.N. Wan, X.Q. Li, G.H. Zhang, J.X. Chen, and T.S. Fan, Plasma Phys. Control. Fusion **60**, 095004 (2018).

<sup>25</sup>S. Agostinelli, Nucl. Instruments Methods Phys. Res. A **506**, 250–303 (2003).